www.serd.ait.ac.th/reric

Thermal and Electrical Performance of Hybrid Photovoltaic-Thermal Collector

A.A. Ghoneim*[1], M.Y. Aljanabi*, A.Y. Al-Hasan[+] and A.M. Mohammedein*

Abstract – This paper presents the results of an experimental investigation of the thermal and electrical yield of a combined photovoltaic-thermal collector in Kuwait climate. The combined photovoltaic-thermal collector is constructed by connecting a conventional PV-laminate to the absorber plate of a conventional flat plate collector. The proposed combination can offer economical advantages compared to a combination of separate thermal and photovoltaic panels. Linear regression analysis was implemented to determine the thermal and optical parameters of the combined collector. The performance measurements indicated that the combined photovoltaic-thermal collector produces a higher yield per unit area than a conventional thermal collector. In order to predict the performance of combined photovoltaic-thermal collector, a numerical model has been developed, consisting of an optical and a thermal model. The well-known flat plate collector formulas have been modified to take into account the effects of adding solar panels. The simulation results of the present work agree well with the experimental data.

1. INTRODUCTION

World energy demand has been significantly increased in the last years due to the world economic growth and population increase, especially in developing countries. The potential for reduction of greenhouse gases emissions is an important issue for the wide spread of renewable energy systems. Solar energy is a clean and renewable energy source, which produces neither green-house effect gases nor hazardous wastes through its utilization. Wide installation of renewable energy systems helps to keep our environment clean and healthy. A combined photovoltaic-thermal collector (PVT) is considered as one of the most interesting applications of solar energy. The combined collector system consists of a photovoltaic laminate that functions as the absorber of a thermal collector. In this situation, the PV panel operates more efficiently since it operates at a lower temperature. The created combined device can convert solar energy into both electrical and thermal energy and both hot water and electricity are produced simultaneously.

The combined photovoltaic-thermal collector (PVT) offers economical advantages compared to a combination of separate thermal and photovoltaic panels. There are certain components as the supporting frame and transparent cover which are common in thermal and photovoltaic panels, but they are shared in combined system. The integration of PV and thermal collector into one system changes the characteristics of both systems. The thermal yield of the solar collector is varied by the increased heat transfer resistance between the absorber

and the fluid. Also, the electrical yield of the solar cells is influenced by the collector flow temperature.

Compared with the conventional collectors, the advantages of the hybrid system are: saving in space, lower operating temperature, and the increase in overall efficiency with simultaneous electricity generation and service water heating. Reducing the temperature of the PV modules to a lower level also increases the effective life of the PV modules as well as stabilizing the current-voltage characteristic curve of the solar cells. The solar cells act as good heat collectors and are fairly good selective absorbers. In addition, in a hybrid PVT system the natural or forced circulation of a heat removing fluid can be used not only for PV cooling but also for heat generation. In this way, the absorbed solar energy which is not converted into electricity can also be utilized for thermal applications.

There are many research works in literature carried out in either thermal or photovoltaic collectors separately. However, in comparison, a little work has been done on the combined system. Combined PVT systems have been studied both analytically and experimentally by a number of researchers. Garg and Agarwal [1] studied a hybrid system with its solar cells used in a compound parabolic concentrator type collector operated in thermosyphon system. The actual optical and thermal performance of PVT system has been presented in reference [2]. Tiwari and Sodha [3] developed a thermal model of an integrated photovoltaic and thermal solar system.

Tripanagnostopoullos *et al.* [4] have examined experimentally a hybrid system and found that the addition of a booster diffuse reflector increases the performance of the system giving possibilities for more interesting practical applications. The thermal models accompanying these studies were basically for steady state analysis.

Jones and Underwood [5] pointed out that a steady state model of the PV module temperature cannot be justified during the periods of rapidly fluctuating irradiance, when the response time caused by the thermal

———————————————————

* Applied Sciences Department, College of Technological Studies, P.O. Box 42325, Shuwaikh 70654, Kuwait.

[+] Electronic Engineering Department, College of Technological Studies, P.O. Box 42325, Shuwaikh 70654, Kuwait.

[1] Corresponding author;
Tel: + 965 66215045, Fax: + 965 483819 6.
E-mail: aa.ghoneim@paaet.edu.kw

mass of the PV material becomes significant. Coventry and Lovegrove [6] carried out a study to compare the value of electrical and thermal output from a domestic PV-thermal system. They concluded that the ratio between the value of electricity and thermal energy plays an important role in minimizing the energy cost of the PV-thermal system.

A combined PV-thermal collector based on a polymer channel absorber plate has been examined [7]. Bakker *et al.* [8] studied a two absorber PV thermal collector. Thermal modeling of a combined system of photovoltaic thermal (PV/T) solar water heater was carried out [9]. Aste *et al.* [10] developed a model to predict the thermal and electrical performance of PVT collector. Their model can be utilized for any set of design and operational parameters for evaluating the performance of PVT air collector.

Coventry [11] measured the performance of a parabolic trough photovoltaic/thermal collector with a geometric concentration ratio of 37 wherein a thermal efficiency around 58% and electrical efficiency around 11%, therefore a combined efficiency of 69% has been recorded. Chow *et al.* [12] constructed an aluminum-alloy flat-box type PVT collector for domestic water heating purpose, with its fin efficiency equal to unity. Their test results showed that a high hot water temperature in the collector system can be achieved after a one-day exposure. They concluded that this equipment is capable of extending the PV application potential in the domestic hot water applications.

A hybrid solar system with high temperature stage is described in [13]. The system contains a radiation concentrator, a photovoltaic solar cell and a heat engine or thermoelectric generator. The possibilities of using semiconductor materials with different band gap values are analyzed. Their calculations showed that the proposed hybrid system is practical and efficient.

Assoa *et al.* [14] developed a simplified steady-state two-dimensional mathematical model of a PVT bi-fluid (air and water) collector with a metal absorber. Then, a parametric study is undertaken to determine the effect of various factors such as the water mass flow rate on the solar collector thermal performances.

Tripanagnostopoulos [15] presented a new type of PVT collector with dual heat extraction operation, either with water or with air circulation. This system is suitable for building integration, providing hot water or air depending on the thermal needs of the building. The modified dual PVT collectors achieved a significant increase in system thermal and electrical energy output.

The present work investigated the thermal and electrical yield of a combined photovoltaic-thermal collector in Kuwait climate. The collector test facility installed at the College of Technological Studies, Kuwait was adapted to carry out the present measurements. In addition, a numerical model is implemented to simulate the performance of the combined collector. The well-known Hottel and Whillier [16] flat plate collector formulas have been modified to take into account the effects of adding the PV modules.

2. EXPERIMENTAL SET-UP

A schematic diagram of the combined photovoltaic-thermal collector configuration chosen for the present study is presented in Figure 1. The hybrid system was constructed by pasting a PV laminates containing multi-crystalline silicon cells (Shell PowerMax Plus 50) into the absorber plate of a conventional glass covered sheet and tube flat plate collector. A thin layer of silicon adhesive was used to paste the PV laminates into the absorber plate.
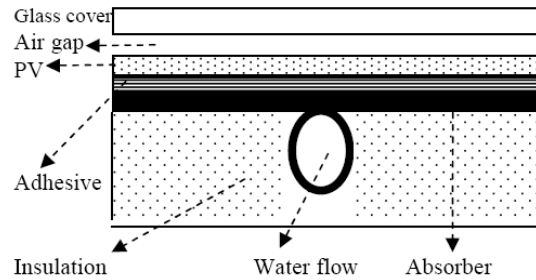
Fig. 1. Schematic diagram of PVT collector.

The combined system was then integrated into the test rig installed on the roof of the main building at the College of Technological Studies, Kuwait. The collector test facility consists of a solar collector, storage tank of 100 liters capacity, cross flow heat exchanger, constant temperature circulator and a circulator pump to overcome the pressure resistance of the system. Several non-return valves were fitted in the pipeline to define the flow direction and a control valve was used to regulate the flow rate through the circuit with the aid of a valve in the pump by-pass line. Filters, pressure relief valve and an air bleed valve were also included in the circuit.

The closed-loop circuit was equipped with both a cross flow heat exchanger and a constant temperature circulator, to control the inlet fluid temperature to the collector. The Haake (model DC50) heating/cooling circulator is capable of supplying water at operating temperature ranges from –50 to 200 °C with accuracy of ±0.01°C. The heat exchanger was used for low inlet fluid temperature experiments.

The solar collector has an aluminum frame of 2x1x0.1 m and was inclined 30° on the horizontal. The collector is constructed from 0.5-mm thick copper absorber plate coated with black paint. Eight copper tubes of 12.5-mm outer diameter were distributed and bonded to the absorber plate. These tubes were between two copper headers made of 42 mm outer diameter. The bottom and sides of the collector were lagged by thermal insulation of 40-mm thickness to reduce back and edge heat losses. A clear white, low iron glass sheet of 6-mm thick was used as a cover with an air gap of about 60-mm thickness left between the absorber plate and the glass cover.

The solar panels consist of 72 encapsulated multi-crystalline silicon cells with a low iron glass front and can generate a peak power of 100 watts. The air gap between the PV laminates and the outer glass cover of the flat plate collector is approximately 20 mm. A set of resistances were used to measure the current-voltage characteristics of the solar panels. The electrical output of the PV panels were connected to a data acquisition system.

The intensity of the global and diffuse solar radiation incident on the collector surface (30° tilted) were measured and recorded by two Eppley Precision Spectral Pyranometers (PSP model) connected to the data acquisition system. The pyranometer used to measure the diffuse solar radiation was fitted with a shading ring such that the detector is shielded from direct solar radiation to measure the diffuse radiation only. During tests, the diffuse radiation was made sure to not exceed 20% of the total radiation incident on the collector surface [17].

Three standard resistance thermometer detectors (RTD-PT100) were used to monitor the surrounding ambient temperature, inlet and outlet fluid temperatures of the collector. This guarantees high accuracy for these critical temperatures. It is to be noted that the RTD sensor of the ambient temperature is shaded from direct and diffuse solar radiation. Ten pre-calibrated type-K thermocouples were distributed on the absorber plate to determine the longitudinal and transversal temperature distribution. Another thermocouple of the same type was used to measure the glass temperature. All temperature sensors were connected to the data acquisition system.

The water flow rate through the collector was measured using a turbine meter suitable for 0.2 to 5 liters/min with accuracy of 3%. The flow meter was outfitted with both digital display and analogue output of 0-5V, which is connected to the data acquisition system.

A data acquisition system (Keithley Model 2700 Multimeter/Data Acquisition) capable of recording 40 channels was used to record the instantaneous measurements of solar intensities, fluid temperatures, ambient temperature, flow rates and electrical output of the PV panels. The data acquisition system has a resolution better than 0.01°C for thermocouple readings and for 4-wires RTD readings.

3. EXPERIMENTAL PROCEDURE

A number of initial tests were performed first to examine the durability and reliability of the collector against extreme conditions. These tests were static pressure test, high temperature stagnation test, thermal shock/water spray test and collector time constant test. Such tests were performed according to the certification of operation issued by Florida Solar Energy Center [18].

The experimental work incorporates measuring the performance of both the conventional flat plate solar collector and the performance of the combined PVT collector. The experiments were carried out for global solar radiation between 650 and 1000 W/m^2, on a 30°-tilted collector surface with average ambient temperatures from 30 to 40°C. The water flow rate of all the experiments ranges from 1.25 to 2.0 kg/min and the inlet water temperature is changed from around the ambient temperature up to 80°C in 10°C steps.

The experimental procedure was started by flushing the system. Then, the system was filled with water and the flow rate was adjusted to the required value. The predetermined inlet fluid temperature was fixed using the cross flow heat exchanger and the constant temperature circulator. The solar collector was allowed to run for over 30 minutes (about 5 times the collector time constant) to achieve quasi-steady-state conditions before the data

collections were started. The data acquisition system records all readings of ambient, fluid and plate temperatures, flow rate, and global and diffuse solar intensity every minute. Each experiment continued for 90 minutes, after that the inlet fluid temperature is changed and a new experiment is started until the set of runs is completed for this arrangement. It should be mentioned that the experiments were performed before noon and repeated after noon to provide similarity around the solar noon. This would minimize the collector heat capacity effect [19].

The collected data were examined to ensure that it presents quasi steady state conditions according to the recommendations outlined by ASHRAE [17]. Then, the concluded data were divided into test periods, each of which is 15 minutes (more than double the collector time constant). The yield of the collector is defined as the amount of useful energy produced by the collector. Knowing the inlet (T_i) and the outlet fluid (T_o) temperatures and the mass flow rate of water ($\dot{m}$), the useful energy (Q_u) gained by the collector can be represented as:

$$Q_u = \dot{m}\, c_p\, (T_o - T_i) \tag{1}$$

where c_p is the specific heat of the working fluid.

On the other hand, the collector thermal efficiency was defined as the yield divided by the amount of solar energy received by the collector. So, the collector thermal (η_{th}) and electrical efficiency (η_{PV}) can be expressed by the following equations:

$$\eta_{th} = \frac{Q_u}{A_c G} = \frac{\dot{m}\, c_p\, (T_{out} - T_{in})}{A_c G} \tag{2}$$

$$\eta_{PV} = \frac{V_{mp} I_{mp}}{A_c G} \tag{3}$$

where A_c is the combined collector area, V_{mp} and I_{mp} are the voltage and current at maximum power point and G is the global radiation on the collector surface.

In the present model, the photovoltaic conversion efficiency is modeled as a linear function of the cell temperature (T_{PV}) in the form:

$$\eta_{PV} = \eta_{ref}\,[1 - \mu(T_{PV} - T_{ref})] \tag{4}$$

where η_{ref} and T_{ref} are the efficiency and the cell temperature at a reference condition and μ is the PV efficiency temperature coefficient.

The amount of solar energy absorbed by the combined collector (Q_u) is reduced since the electrical energy is extracted from the solar cells. The electrical efficiency, which is a function of the temperature, is subtracted from the transmission-absorption coefficient to find the thermal efficiency of the hybrid collector:

$$\eta_{th} = F_R\,(\tau\alpha - \tau\eta_{PV}) - F_R\, U_L\, \frac{(T_i - T_a)}{G} \tag{5}$$

where $\tau\alpha$ is the transmittance-absorptance product, T_a is the ambient temperature, U_L overall heat loss coefficient and η_{PV} is the PV efficiency. The heat removal factor (F_R)

was calculated from the well-known Hottel-Whillier equations [19].

4. THEORETICAL MODELS

Two models were required to determine the performance of the combined PVT collector. The first model is an optical model and is required to determine how much irradiation is absorbed by the PVT collector. The optical model was used to calculate the transmission-absorption coefficient of the PVT collector ($\tau\alpha$) and this value was then inserted as a constant into the thermal model. The second model is required to determine the heat flows within the PVT collector.

Optical Efficiency

The optical model adapted for the present study is based on the net radiation method. The net radiation method solves the energy flux balance at each interface in the PVT collector configuration. The values for the coefficients of reflection are determined from the well known Fresnel equations. This method is applied to all the interfaces in the PVT collector which generates a set of equations that is can be solved by matrix methods. Since both the coefficient of extinction (K) and the index of refraction (n) depend on the wavelength, the equations are solved for each wavelength interval separately and then integrated over the solar spectrum. The present calculations are based on the assumption of specular reflection, so diffuse reflection is not taken into consideration.

However, the PV laminate introduces more complication to the problem as the PVT laminate does not present a homogeneous surface but consists of different parts. These parts are active PV area, the top grid and the spacing between the cells. For each part, the value for ($\tau\alpha$) was calculated separately and then ($\tau\alpha$) of the entire PVT collector was evaluated by taking the average of these values, weighed with the respective surface areas. The average value of ($\tau\alpha$) was found to be approximately equal to 0.68. The average value of ($\tau\alpha$) was then inserted into the thermal model to calculate the overall thermal efficiency of the combined collector.

Thermal Efficiency

The thermal model is a steady state model based on solving the heat balance equations for all the layers in the PVT collector. The average value of the transmittance-absorptance product ($\tau\alpha$) which is 0.68 was then inserted into the thermal model. The electrical efficiency, which is a function of the temperature, is subtracted from the transmission-absorption coefficient to find the thermal energy that was absorbed by the system. So, the amount of solar energy absorbed by the combined collector (Q_u) is reduced since electrical energy is extracted from the solar cells. Thus, one can obtain the amount of absorbed energy that contributes to the thermal yield as:

$$Q_u = GA_c \, (\tau\alpha - \tau_{PV} \, \eta_{PV}) \qquad (6)$$

The transmittance-absorptance product ($\tau\alpha$) was assumed to be the same for the absorber plate and the PV cells. The heat flows through the combined collector can

be represented by a set of heat energy balance equations. The heat removed by the water (Q_u) is given by:

$$Q_u = Q_{PVp} - Q_{ba} \qquad (7)$$

where Q_{PVp} is the heat flow from PV cells to the absorber plate, and Q_{ba} is the heat transferred from collector back to the ambient. Since an adhesive layer is used to connect the PV laminate to the absorber, then the heat transfer between the PV cells and the absorber can be expressed as:

$$Q_{PVp} = h_{PVp} \, (T_{PV} - T_p) \qquad (8)$$

$$Q_{ba} = h_{ba} \, (T_p - T_a) \qquad (9)$$

where h_{ba} and h_{PVp} is the heat transfer coefficient from collector back to the ambient and from PV laminate to absorber plate, respectively.

The heat energy balance at the different layers of the combined photovoltaic thermal collector also gives:

$$Q_{PVp} = (\tau\alpha - \tau_{PV}\eta_{PV}) \, G - Q_{PVg} \qquad (10)$$

$$Q_{PVg} = Q_{conva} + Q_{rada} \qquad (11)$$

$$Q_{conva} + Q_{rada} = Q_{gt} \qquad (12)$$

$$Q_{gt} = Q_{convs} + Q_{rads} \qquad (13)$$

$$Q_{rads} = F_s \varepsilon_g \sigma (T_{gtup}^4 - T_s^4) + F_e \varepsilon_g \sigma (T_{gtup}^4 - T_a^4) \quad (14)$$

$$Q_{convs} = h_w \, (T_{gtup} - T_a) \qquad (15)$$

$$Q_{rada} = \frac{\varepsilon_g \varepsilon_{PV}}{\varepsilon_g + \varepsilon_{PV} - \varepsilon_g \varepsilon_{PV}} \sigma (T_{PVg}^4 - T_{gtdown}^4) \qquad (16)$$

$$Q_{conva} = h_a \, (T_{PVg} - T_{gtdown}) \qquad (17)$$

$$Q_{PVg} = \frac{k_g}{\Delta x_{PVg}} \, (T_{PV} - T_{PVg}) \qquad (18)$$

$$Q_{gt} = \frac{k_g}{\Delta x_{gt}} \, (T_{gtdown} - T_{gtup}) \qquad (19)$$

All previous notations are defined in the nomenclature.

The thermal resistance of the different layers of material between the solar cells and the copper absorber is minimized by using highly conductive glue. The heat transfer coefficient (h_{PVp}) was calculated by measuring the temperature difference between the glass surface of the solar cells and the absorber. The average absorber temperature (T_p) was calculated from the temperature distribution formula [19]. A numerical technique was developed to solve the heat energy balance equations to obtain the unknown temperatures required to determine the thermal and electrical performance of PVT collector.

5. EXERGY EFFICIENCY

The overall performance of PVT can be evaluated by the first law efficiency (η_{PVT}) which is equal to thermal and electrical efficiency. Thermal energy cannot produce work

until a temperature difference exists between a high temperature heat source and a low temperature heat sink, whereas electrical energy can completely transform into work irrespective of the environment. So, the fist law efficiency is not comprehensive for evaluating the PVT overall performance. Exergy (ψ_{PVT}) is defined as the available energy obtained by subtracting unavailable energy from total energy and is equivalent to the work transformable. The use of exergetic efficiency (second law efficiency) thus enables qualitative evaluation of PVT overall performance by comparing electrical and thermal energy based on the same standard. The overall energy efficiency of PVT collector assuming a thermal conversion factor of 0.38 is given by [20]:

$$\eta_{PVT} = \frac{\eta_{PV}}{0.38} + \eta_t \qquad (20)$$

The exergy efficiency is defined as the ratio of total exergy output to total exergy input [21]. The exergy efficiency of PVT collector (ψ_{PVT}) can be expressed as [21]:

$$\psi_{PVT} = \eta_{PV} + \eta_t [1 - \frac{T_o}{T_o + (T - T_a)}] \qquad (21)$$

6. ENVIRONMENTAL LIFE CYCLE ASSESSMENT

The amount of fossil CO_2 emission avoided by using a renewable resource instead of a fossil fuel power generation technology depends on the fossil fuel type that is avoided, and on the conversion technology used to make the power from that fossil fuel. Replacing a higher CO_2 emitting plant with a lower or non CO_2 emitting plant results in decreased CO_2 addition to the environment. This difference in the amount of CO_2 emitted is referred to as CO_2 avoided emission. The CO_2 emission avoided is generally defined as the difference between emissions generated by conventional systems and emissions generated in the production of the PV system over the life time of the system (25 years). A theoretical model was developed to calculate the CO_2 avoided emission achieved by using combined photovoltaic-thermal collector system to satisfy the needs of a family in a typical Kuwaiti house from domestic hot water load and electricity consumption (lighting and household appliances).

Emissions generated in the production of the PVT system are much less than the emissions generated by conventional systems and can be neglected [22]. In the present analysis, avoided CO_2 emission (E_A) (in tonne CO_2) is mainly the CO_2 emissions which generated by conventional systems and can be expressed by the following expression:

$$E_A = P_g \times F_E \qquad (22)$$

where P_g is the power generation (kWh) and F_E is the plant emission factor (tonne CO_2 /kWh).

To perform CO_2 emission reduction analysis for the PVT system, one needs to define the baseline (also called base case or reference case) electricity system. Often this will simply imply defining a conventional system and its associated fuel (oil, natural gas, coal). The default

emission factors and conversion efficiencies of various fuel types [23] are input to the model in each case. The model can calculate the CO_2 emission reduction for each reference fuel type.

7. RESULTS AND DISCUSSIONS

The experimental results are presented in forms of graphs that present the collector efficiency variation against the reduced temperature parameter $(T_i - T_a)/G$. All the presented data grant a quasi steady state for each test period (The test period is the duration in which 15 data points are averaged and shown as a single point in the presented results). This is confirmed by the fact that, within the test period (15 min), the maximum variations in ambient, inlet and outlet temperatures are ± 0.5 °C, ± 0.1 °C and ± 0.3°C, respectively, while in global radiation is $\pm 16 W/m^2$. Also, diffuse radiation did not exceed 15% of global radiation in any experiment [17].

To examine the reliability of the present developed numerical model, the calculated performance of the combined PVT is compared to the corresponding performance obtained from the experimental data. For the sake of clarity, the linear curves only obtained from linear regression analysis of the experimental data are presented in Figure 2 along the theoretical values. The values of $F_R(\tau\alpha)$ and $F_R U_L$ for PVT collector obtained from measurements are 0.55 and 5.8 which agree well with the values of 0.58 and 6.0 predicted by the theoretical model. The results clearly confirm the reliability of the present numerical model as the theoretical predictions agree well with the experimental data. The maximum difference between the two predictions is less than 5%.
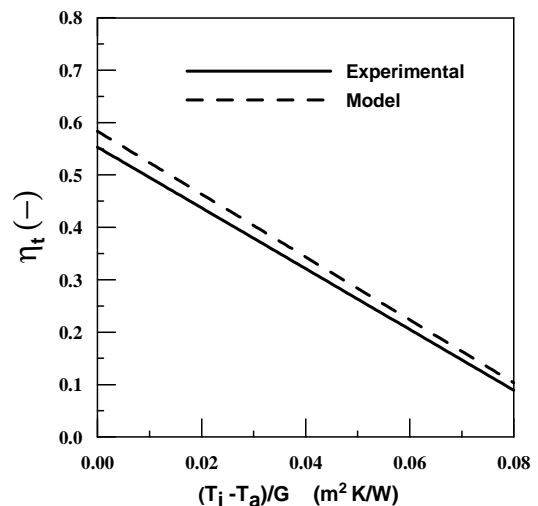
Fig. 2. Calculated and measured PVT efficiency.

To evaluate the performance of the combined PVT collector, its performance was compared to the performance of the conventional thermal collector. Figure 3 shows the variation of thermal efficiency with the reduced temperature parameter $(T_i - T_a)/G$ for the conventional thermal collector and the combined PVT collector. The average points of the experimental data are shown in the figure. The scatter of the data around the straight line is mainly attributed to the angle of incidence variations, wind speed and the dependence of U_L on the

plate temperature. Also, the variations of the relative proportions of beam, diffuse and ground reflective components of solar radiation are participating in the data scattering, so scatters in the data are expected.
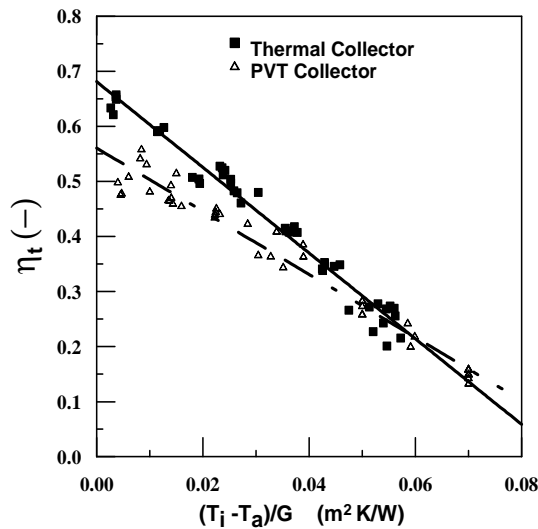
Fig. 3. Comparison between PVT and T collector.

Linear regression analysis was adapted to fit the experimental data to linear curves for both cases. The line intersection with the y-axis gives $F_R (\tau\alpha)$, while the value of the parameter $F_R U_L$ is equal to the slope of the line. Table 1 presents the values of the parameters $F_R (\tau\alpha)$ and $F_R U_L$ for both combined (PVT) and conventional thermal (T) collector along the variance (R^2) obtained from the regression analysis.

Table 1. Thermal efficiency parameters for collectors.

Collector	$F_R(\tau\alpha)$	$F_R U_L$	R^2
PVT	0.55	5.8	0.96
T	0.67	8.3	0.97

The value of $F_R U_L$ of PVT collector was reduced by about 30% compared to the value of conventional thermal collector. On the other hand, the optical efficiency of the combined collector is reduced by about 18% only. These results show the significant improvement accomplished when using combined photovoltaic thermal collector.

It is worth to mention that the effect of optical efficiency is dominant at low temperature difference, whereas the effect of heat loss is important at high temperature difference. Thus, the efficiency of the combined collector is better than the efficiency of the conventional thermal collector particularly at medium and high temperatures. On the other hand, the conventional thermal collector gives better efficiency for limited low temperature range.

The relative effect of PV electrical output on η_{th} was examined by running PVT system with the PV modules in an alternating on/off cycle. The resulting thermal energy is plotted versus reduced temperature as shown in Figure 4. Figure indicates that extracting electrical energy from the PV panels reduces the solar energy absorbed by the combined collector, and consequently reduces the thermal efficiency of the combined collector by approximately 12% as predicted from the figure.
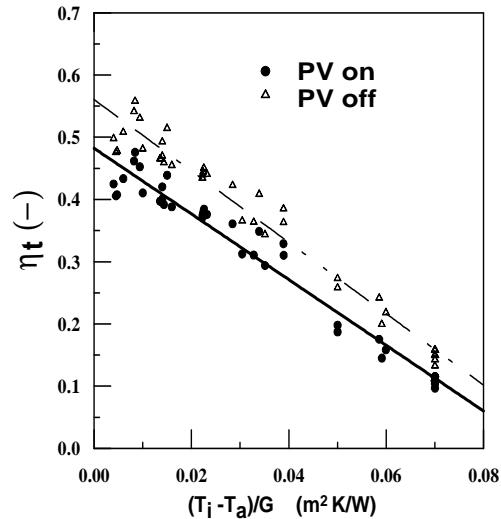
Fig. 4. Thermal efficiency of PVT collector with and without PV power output.

The photovoltaic efficiency (η_{PV}) is calculated from the measured voltage over a set of standard resistances. The I-V characteristics of the PV laminate at 55°C and 25°C is presented in Figure 5. The figure clearly illustrates the effect of cooling on the photovoltaic output. Increasing the cell temperature decreases the open circuit voltage (V_{oc}). That is can mainly attributed to the diode reverse saturation current which increases exponentially with temperature [24]. So, the most significant effect of the PVT collector is the cooling effect for the solar cells. This fact puts an upper limit on the system temperature, which must be considerably lower than the desired cell temperature. Thus the PVT collector can be used successfully in systems that demand a relatively low operating temperature as domestic hot water systems.
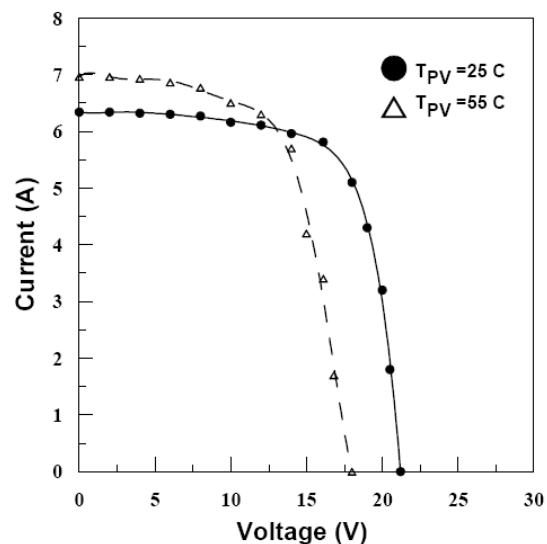
Fig. 5. IV characteristics of PV laminate at different temperatures.

A comparison is carried out between the energy efficiency (first law) and exergy performance (second law) to study the effect of different parameters on the overall performance of PVT collector. As an example, the variation of overall energy efficiency (η_{PVT}) and overall exergy efficiency (ψ_{PVT}) with solar radiation is presented

in Figure 6. It is obvious that the increase in solar radiation leads to a decrease in overall energy efficiency but at the same time it leads to increase in overall exergy efficiency of the combined PVT collector. In general, it is observed that if a parameter change is favorable for the thermal exergic efficiency, then it is unfavorable for the photovoltaic exergic efficiency.
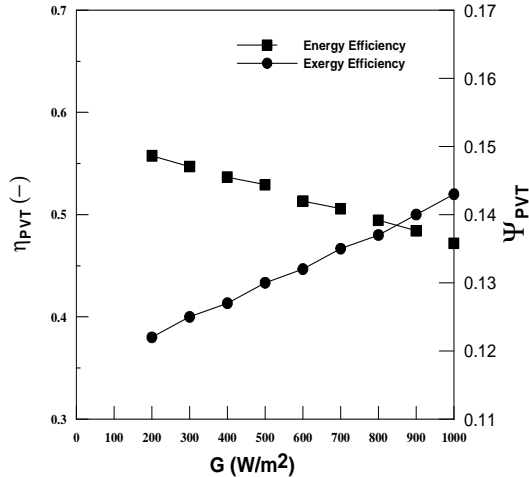
Fig. 6. Variation of overall efficiency with solar radiation.

The uncertainty analysis shows an experimental error of about 0.8, 1.3, 2.4, 3.4, 3.9 and 5.1% for $F_R U_L$, $F_R(\tau\alpha)$, (η_t) (η_{PV}), (η_{PVT}), and (ψ_{PVT}), respectively. The uncertainty analysis for the experimental data revealed that the optical efficiency $(\tau\alpha)$ is more sensitive to experimental error than the heat loss coefficient, U_L. The total experimental error for the collector thermal efficiency (η_t) and the photovoltaic efficiency (η_{PV}) is calculated based on the calculation of the combined error from all measured parameters.

The recovered heat energy from the hybrid PVT collector is assumed to satisfy the needs of a family in a typical Kuwaiti house from domestic hot water load and electricity consumption (lighting and household appliances). Assuming a figure of 40 liters/person/day, the hot water demand is 280 liter/day. The electrical load in the house is the total energy consumption in the house. The computer program is provided with an estimate of typical loads encountered in the house. The two-story house consists of two living rooms, six bedrooms, dining room, two kitchens and a set of household appliances (refrigerator, kitchen machine, vacuum cleaner, etc). An hourly load schedule, which repeats each day, is written to a file to be called during calculation. The program is provided with an estimation of the number of hours that the load is used during a typical day for each household appliance.

Different photovoltaic-thermal collector slopes and azimuth angle were studied to maximize the annual energy generated by the combined PVT system. The maximum energy generation from the combined PVT collector corresponds to a collector slope of 25° (Kuwait latitude-5°) and facing south (azimuth angle=0°). Maximum energy production at angles less than location latitude is coincident with the fact that more solar energy is available in summer than in winter in Kuwait.

The accurate analysis of the total avoided emissions for PV systems, should take into account the emission generated in the fabrication phase of the PVT system components. The CO_2 emission rate from PVT systems is much lower than the CO_2 emission rate from conventional utility and can be neglected.

The variation of annual avoided CO_2 emission with tilt angle is presented in Figure 7. The figure again illustrates that the optimum tilt angle which maximizes the avoided CO_2 emission is 25°. At this optimum angle, the avoided CO_2 emission is approximately equals to 1.4 tonne/year which confirms the environmental impacts of the PVT collector.
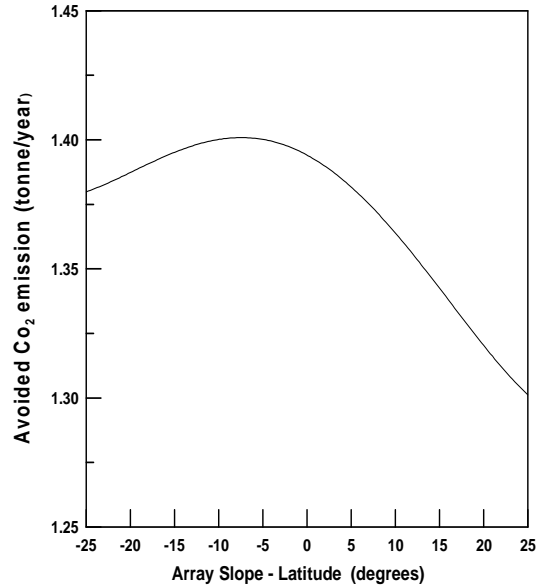
Fig. 7. Avoided CO_2 emission variation with array slope (azimuth angle=0).

In addition, the costs due to the application of the Kyoto Protocol, which penalizes the emissions of green house effect gases, fundamentally CO_2, should be added to the costs of conventional energy resources. In spite of the fact that Kyoto Protocol is not currently applied in Kuwait, however considering application of this protocol will enhance the economical and environmental aspects of PVT systems much more.

7. CONCLUSIONS

A PV laminate has been pasted on the absorber of a conventional thermal collector to construct a combined PVT collector. The combined PVT collector was integrated on a test rig to examine its performance. A numerical model was developed to verify the experimental results obtained. Based on the present results, the following conclusions can be drawn out:

- The available solar energy for the thermal system is reduced since a part of the incident radiation is converted to electricity by the PV cells.
- The PVT collector reduces the heat loss coefficient significantly and this reduction is more important than the loss in optical efficiency.
- The performance of the PVT collector is better than that of conventional one due to the lower heat loss coefficient.

- Extracting electrical energy from the PV panels reduces the thermal efficiency of the combined collector by approximately 12%.
- Maximum energy generation from the PVT collector corresponds to a collector slope of 25° (Kuwait latitude-5°) and facing south (azimuth angle=0°).
- The combined PVT collector produces a higher yield per unit area than a thermal collector and a PV laminate placed next to each other.
- The PVT collector can be used successfully in systems that demand a relatively low temperature as domestic hot water systems.
- At the optimum conditions, an avoided CO_2 emission of approximately 1.4 tonne/year can be achieved which confirms the environmental impacts of the PVT system.
- Exergy is a useful tool which can be used in the assessment of overall performance of hybrid PVT collector.

ACKNOWLEDGEMENT

NOMENCLATURE

A_c	collector area (m^2)
c_p	specific heat of working fluid (J/kgK)
E_A	avoided CO_2 emission (tonne CO_2)
F	view factor (-)
F_E	plant emission factor (tonne CO_2 /kWh)
F_R	heat removal factor (-)
G	global solar radiation (W/ m^2)
h_{ba}	heat transfer coefficient from collector back to ambient (W/ m^{2}K)
h_{PVp}	heat transfer coefficient from PV laminate to absorber plate (W/ m^{2}K)
h_w	wind heat transfer coefficient (W/ m^{2}K)
I_{mp}	current at maximum power point (A)
k_g	thermal conductivity of glass (W/mK)
$\dot{m}$	mass flow rate of water (kg/s)
P_g	power generation (kWh)
Q_{ba}	heat transferred from collector back to ambient (W)
Q_{conva}	heat transferred by convection in air gap (W)
Q_{convs}	heat transferred by convection to sky (W)
Q_{gt}	heat transferred from the upper surface of the glass cover (W)
Q_{rada}	heat transferred by radiation in air gap (W)
Q_{rads}	heat transferred by radiation to sky (W)
Q_{PVg}	heat flow from PV cells to glass (W)
Q_{PVp}	heat flow from PV cells to absorber plate (W)
Q_u	useful energy gained by PVT collector (W)
T_a	ambient temperature (°C)
T_{gtdown}	temperature of the lower surface of the glass cover (°C)
T_{gtup}	temperature of the upper surface of the glass cover (°C)
T_{in}	collector inlet temperature (°C)

T_{out}	collector outlet temperature (°C)
T_o	reference ambient temperature (K)
T_P	absorber average temperature (°C)
T_{PV}	solar cell temperature (°C)
T_{PVg}	temperature of the PV glass (°C)
T_{ref}	temperature of PV cell at reference temperature (°C)
T_s	sky temperature (K)
U_L	overall heat loss coefficient (W/ m^{2}K)
V_{mp}	voltage at maximum power point (V)

Greek Letters

Δx_{gt}	glass cover thickness (m)
Δx_{PVg}	PV laminate thickness (m)
ε_g	glass cover emissivity (-)
ε_{PV}	PV cell emissivity (-)
η_{PV}	electrical efficiency of the PV cells (-)
η_{ref}	efficiency at reference condition (-)
η_t	collector thermal efficiency (-)
η_{PVT}	overall PVT thermal efficiency (-)
ψ_{PVT}	overall PVT exergy efficiency (-)
μ	PV efficiency temperature coefficient (°C^{-1})
σ	Stefan-Boltzmann constant (W/m^{2}K^4)
$\tau\alpha$	transmission-absorptance coefficient without PV power output (-)
$(\tau\alpha)_{PV}$	transmission- absorptance coefficient of pure PV module (-)

REFERENCES

[1]   Garg, H.P. and Agarwal, R.K. 1995. Some aspects of a PV/T collector: forced circulation flat plate solar water heater with solar cells. *Energy Conversion and Management* 36: 87-99.

[2]   Krauter, S. and Hanitsch, R. 1996. Actual optical and thermal performance of PV modules. *Solar Energy Materials and Solar Cells* 41: 557-574.

[3]   Tiwari, A. and Sodha, M.S. 2006. Performance evaluation of solar PV/T system: An experimental validation. *Solar Energy* 80: 751-759.

[4]   Tripanagnostopoullos, Y., Nousia, T.H., Souliotis M., and Yianoulis, P. 2002. Hybrid photovoltaic/thermal solar systems. *Solar Energy* 72: 217-234.

[5]   Jones, A.D. and Underwood, C.P. 2001. A thermal model for photovoltaic systems. *Solar Energy* 70: 349-359.

[6]   Coventry, J.S. and Lovegrove, K. 2003. Development of an approach to compare the value of electrical and thermal output from a domestic PV/thermal system. *Solar Energy* 75: 63-72.

[7]   Sandnes, B. and Rekstad J. 2002 A photovoltaic/thermal (PV/T) collectors with a polymer absorber plate-experimental study and analytical model. *Solar Energy* 72: 63-73.

[8]   Bakker, M., Zondag, H.A. and Van Helden, W.G.J. 2002. Demonstration on a dual flow photovoltaic/thermal combi-panel. *Proceedings of PV in Europe-From PV Technology to Energy Solutions*. Conference and Exhibition, October 7-11; Rome, Italy.

[9]   Dubey, S. and Tiwari, G.N. 2008. Thermal modeling of a combined system of photovoltaic thermal (PV/T) solar water heater. *Solar energy* 82: 602-612.

[10] Aste, N., Chiesa, G. and Verri. 2008. Design, development and performance monitoring of a photovoltaic-thermal (PVT) air collector. *Renewable Energy* 33: 914-927.

[11] Coventry, J.S. 2005. Performance of a concentrating photovoltaic/thermal solar collector. *Solar Energy* 78: 211-222.

[12] Chow, T.T, He, W. and Ji, J. 2006. Hybrid photovoltaic-thermosyphon water heating system for residential application. *Solar Energy* 80: 298-306.

[13] Vorobiev, Yu., González-Hernández J., Vorobiev P. and Bulat L. 2006. Thermal-photovoltaic solar hybrid system for efficient solar energy conversion. *Solar Energy*; 80:170-176.

[14] Assoa, Y.B., Menezo, C., Fraisse, G., Yezouand, R. and Brau J. 2007. Study of a new concept of photovoltaic–thermal hybrid collector. *Solar Energy* 81: 1132-1143.

[15] Tripanagnostopoulos, Y. 2007. Aspects and improvements of hybrid photovoltaic/thermal solar energy systems. *Solar Energy* 81: 1117-1131.

[16] Hottel, H.C. and Whillier, A. 1958. In evaluation of flat plate collector performance. *University of Arizona Press* 2: 72-104.

[17] ASHRAE. 1986. Methods of Testing to Determine the Thermal Performance of Solar Collectors. *ASHRAE Standard 93-86*. Atlanta, Georgia, USA.

[18] Florida Solar Energy Center. 2002. Operation of the Collector Certification Program. SEC-GP-6-80, Cocoa, Florida 32922-5703.

[19] Duffie, J.A. and Beckman, W.A. 1993. *Solar Engineering of Thermal Process*. New York: Wiley Inter-science.

[20] Joshi, A.S. and Tiwari, A. 2007. Energy and exergy efficiencies of a hybrid photovoltaic-thermal (PV/T) air collector. *Renewable Energy* 32: 2223-224.

[21] Hepbasli, A. 2008. A key review on exergetic analysis and assessment of renewable energy resource for a sustainable future. *Renewable and Sustainable Energy Reviews* 12: 593-661.

[22] Hill, R. and Baumann, A.E. 1993. Environmental Costs of Photovoltaics. *IEE Proceedings* 140:76-80.

[23] Energy Information Administration. 1999. *Emissions of Greenhouse Gases in the United States 1998*, Chapter 2 in "Carbon Dioxide Emissions. 1999. *DOE/EIA-0573(98)*, Washington, DC.

[24] Fahrenbruch, A.L. and Bube R.H. 1983. Fundamentals of Solar Cells, Photovoltaic Solar Energy Conversion, *Academic Press*, New York, 1983.